

RSC Advances



This is an *Accepted Manuscript*, which has been through the Royal Society of Chemistry peer review process and has been accepted for publication.

Accepted Manuscripts are published online shortly after acceptance, before technical editing, formatting and proof reading. Using this free service, authors can make their results available to the community, in citable form, before we publish the edited article. This *Accepted Manuscript* will be replaced by the edited, formatted and paginated article as soon as this is available.

You can find more information about *Accepted Manuscripts* in the [Information for Authors](#).

Please note that technical editing may introduce minor changes to the text and/or graphics, which may alter content. The journal's standard [Terms & Conditions](#) and the [Ethical guidelines](#) still apply. In no event shall the Royal Society of Chemistry be held responsible for any errors or omissions in this *Accepted Manuscript* or any consequences arising from the use of any information it contains.

Biodegradable polyurethane acrylate/HEMA-grafted nanodiamond composites with bone regenerative potential applications: structure, mechanical properties and biocompatibility

Maryam Alishiri, Akbar Shojaei^{*}, Mohammad Jafar Abdekhodaie

Department of Chemical and Petroleum Engineering, Sharif University of Technology,

P. O. Box †11155-9465, Tehran, Iran

Abstract

Present study demonstrated HEMA-grafted nanodiamond (ND-HEMA)/acrylate-terminated polyurethane-Acrylate diluents (APUA) composites as promising materials for bone implants applications. Neat APUA and APUA composites containing ND-HEMA at different loadings up to 2 wt % were prepared by in situ polymerization method. Morphological analysis exhibited that ND-HEMAs were actually in the form of tightly bound aggregate which led to formation of big agglomerates at concentration of 2wt%. It was also suggested that ND-HEMAs were preferentially localized in the continuous soft domain of APUA; however it interacted by both soft and hard domains. Moreover, ND-HEMAs caused considerable phase separation between soft and hard domains as well as increased crystallinity. Maximum improvement in tensile properties of APUA was observed at 1 wt% loading of ND-HEMAs, namely 175% improvement in modulus and 40% increase in strength. Hydrophilic nature of ND-HEMAs enhanced water

^{*}Corresponding author, Tel/Fax: +98 21 66166432.

E-Mail address: akbar.shojaei@sharif.edu (Akbar Shojaei).

absorption of composites resulted in higher hydrolysis degradation of APUA. *In vitro* biocompatibility evaluation via culturing human osteosarcoma cells (MG-63 osteoblast-like cell line), demonstrated no adverse effect on cell viability of samples. Furthermore, composites showed favorable cell adhesion and growth, and ND-HEMAs did not cause any negative effect on proliferation, ALP production and osteoblast attachment by MG-63 cells compared with neat APUA.

Introduction

Polyurethane (PU) and its derivatives such as acrylate-terminated PU(APU) are increasingly used in broad range of biomedical applications especially for bone implants and orthopedic.¹⁻³ This is primarily due to their high flexibility, unique mechanical properties, chemical stability, biocompatibility and aptitude for tailoring physical properties of the target tissue.³ An ideal candidate material for bone repairing must be biocompatible and biodegradable and its mechanical properties and composition should be similar to those of bone.⁴ Major drawbacks in the bone regenerative applications of PUs have arisen from their insufficient mechanical properties, weak durability and rather hydrophobic nature⁵ that must be improved appropriately for load-bearing tissue-replacement strategies.⁶

Incorporation of appropriate functional or reinforcing particles is versatile route to improve the performance of PUs and its derivatives.⁷ Reinforcement of PUs in hard tissue applications has been attempted through incorporating rigid particles such as β -tricalcium phosphate(β -TCP),¹ mineralized allograft bone particles (MBPs)² and hydroxyapatite nanoparticles(nHA)⁸ in the recent decade. However, present functional nanoparticles have been shown to be much influential on the property enhancement of polymer matrices compared to micron sized particles. Amongst many nanoparticles investigated in the field of polymer nanocomposites, nanodiamond

(ND) is increasingly receiving much attention in research community due to its superior mechanical properties (Young's modulus 1220 GPa),⁹ high thermal conductivity,¹⁰ low friction coefficient,¹¹ unique electrical resistivity and optical properties.⁹ These unique characteristics along with the rich surface chemistry with tunable surface,⁴ biocompatibility and low toxicity have made ND favorable candidate for biomedical applications.¹² Additionally, mass production of ND with reasonable price is promising because of availability of economically viable production techniques such as detonation method.¹⁰

Recent studies have shown that ND is able to improve significantly the mechanical, tribological and thermal conductivity of polymers at both low, e.g. ~ 1 wt%¹³ and high, i.e. above 20 wt%,¹⁴ ND loadings. However, the studies on PU/ND nanocomposites dealing with microstructure, mechanical properties and functional performance have been rarely reported in literature. Recent investigation on nanostructure, dynamics and elastic properties of hybrid nanocomposites containing semi-interpenetrating polymer network of PU and poly(2-hydroxyethyl methacrylate) with 3-D diamond exhibited maximal effects at low contents, as low as 0.25 wt%.¹⁰ It was also shown that incorporation of a few percent of ND, e.g. 0.5 wt%, led to a remarkable improvement in tribological properties of elastomeric PU, while its elastic behavior and tensile strength remained almost unchanged.¹⁵

Enhancement of the mechanical properties in the polymer matrix containing ND is rather complicated due to the formation of ND agglomeration,⁴ difficulties in obtaining a homogeneous dispersion of nanoparticles⁸ and challenges in generation of sufficient interfacial adhesion.⁷ The poor interfacial interactions often lead to weak load transferring between hosting polymer and the reinforcements. Therefore, it is necessary to tailor the surface chemistry of NDs according to intrinsic chemical nature of polymer matrix. Consequently, appropriate surface functionalization

of ND along with a suitable mixing method such as melt mixing and in-situ polymerization could be effective in preventing the formation of large agglomerates in polymer/ND composites.¹⁶

Literature shows that the polymer/ND composites targeted for biomedical applications has also been investigated more or less by researchers. Zhang et al.⁴ reported that ND filled poly(L-lactic acid) (PLLA) composite exhibited significantly enhanced mechanical properties and increased biomineralization with no toxicity on murine osteoblast cell (7F2) proliferation which was suggested to be used as bone scaffolds and regenerative medicine. The attempt conducted by Protopapa et al.¹⁷ to increase overall performance of poly methyl methacrylate (PMMA) by ND for fixed interim prostheses was found to be successful.

Recently, we synthesized biodegradable APUs based on low molecular weight poly(ϵ -caprolactone) diol (PCL), aliphatic 1,6-hexamethylene diisocyanate (HDI) and hydroxyethyl methacrylate (HEMA) as potential thermosetting polymers for tissue applications.¹⁸ It was shown that these polymers exhibited complex multiphase microstructure containing soft and hard domains with either amorphous and/or crystalline morphologies which were chemically cross-linked. The objective of the present work was to examine the potential aptitude of ND on the improvement of mechanical properties of biodegradable APU. The attempts were made to explore the structure-properties relationship in such complicated multiphase polymeric system. As the composite was targeted for biomedical applications, its cytotoxicity and *in vitro* degradation properties were also investigated thoroughly.

Materials and methods

1.1. Materials

Poly(ϵ -caprolactone)diol (PCL, CAPA 225 with molecular weight of 2000, Interlox Chemicals), 1,6-Hexamethylene diisocyanate (HDI, Merck Chemical) and 2-Hydroxyethyl methacrylate

(HEMA, Sigma-Aldrich) were obtained to synthesize APU. Mixture of HEMA and ethylene glycol di-methacrylate (EGDMA) from Merck Chemical was used as reactive diluents as well. 2,2-azobisisobutyronitrile (AIBN, Sigma-Aldrich) and thionyl chloride (SOCl_2) (Duksan Pure Chemical, South Korea) were used as received. Detonated ND with an average single particle diameter of 4-6 nm, specific surface area of $282 \text{ m}^2/\text{g}$ and purity of 98-99% was obtained from NaBond Technologies Co., China.

2.2. Functionalization of ND with HEMA

The whole functionalization process, as shown in Scheme 1, consists of three steps, namely, thermal oxidation of ND, followed by acyl-chloride functionalization and finally grafting HEMA onto outer surface of NDs. Thermal oxidation was carried out on as-received NDs under air atmosphere at 420°C in a furnace (S302AU, Carbolite Co., England) for 1.5 h according to literature¹⁹ to convert oxygen-containing groups to carboxylic acid on the ND surface, henceforth referred to as ND-COOH. Then, acyl-chloride grafted ND (hereafter designated as ND-COCl) was synthesized as intermediate product based on ND-COOH similar to methodology mentioned in literature.^{16,20} To do this, ND-COOH was stirred at reflux with thionyl chloride under nitrogen atmosphere at 65°C for 24 h in an excess amount (25 mg ND per 1 ml thionyl chloride). The mixture was cooled down to room temperature and then excess thionyl chloride was removed by filtering and washing with anhydrous THF. A wash cycle consisted of sonicating at 50 W for 1 min in bath-type ultrasonicator followed by 20 min centrifugation at 4000 rpm was repeated until the liquid filtrate came out colorless. Grafting of HEMA onto the surface of ND was carried out by esterification reaction between ND-COCl and HEMA.^{16,21} In a typical experiment, 2 ml of HEMA were mixed with 500 mg of ND-COCl dispersed in 10 ml of anhydrous THF. This mixture was stirred for around 6 h at ambient temperature under nitrogen atmosphere. The resultant functionalized ND was collected and separated by repeated centrifugation and acetone

washing and finally dried under vacuum oven at 40 °C overnight to give the HEMA functionalized ND, henceforth referred to as ND-HEMA.

2.3. Preparation of test specimens

APU was synthesized by PCL:HDI:HEMA with mole ratio of 1:2:2 using a two-step polymerization method described previously.¹⁸This mole ratio is resulted in APU molecule typically containing one PCL core segment attached with two HDI molecules at chain ends which are end-capped with HEMA. Predefined amount of APU oligomer was heated slightly above ambient temperature and then mixed with mixture of two reactive diluents, i.e. mixture of HEMA:EGDMA with weight ratio of 70:30. Mixture of APU and acrylate monomers (reactive diluents) was denoted by APUA in which the weight ratio of APU and mixed acrylate monomers was kept on 70:30. HEMA grafted ND, ND-HEMA, was added into APUA at three different loadings of 0.5, 1 and 2 wt % and then the mixtures were stirred for 2hr. To achieve homogeneous dispersion of ND-HEMA throughout the matrix, the mixture was held under an ultrasound bath for 10 min. Finally, AIBN (1 wt. %) was added to the above mentioned mixtures for initiating crosslinking reaction through the vinyl groups of APUA. After homogenous mixing, the mixture was degassed under vacuum for 5–10 min at ambient temperature and then it was poured into a glass mold. The mold was placed in an oven at 80°C for 3 h to let APUA be crosslinked.

2.4.Characterization

Fourier transform infrared spectroscopy (FTIR) analysis was carried out using ABB Bomem MB100 spectrophotometer (Canada) on a KBr pellet at room temperature. Thermogravimetric Analysis (TGA) was performed using a Mettler Toledo (TGA-DSC 1 model, USA) on samples of 5-10 mg under nitrogen atmosphere with heating rate of 10 °C/min.

The average diameter and size distribution of a very dilute (0.0003 wt%) ND dispersion in chloroform was determined via dynamic light scattering (DLS) on a Malvern Zetasizer Nano S instrument (Red badge), ZEN1600 (Malvern Instruments Ltd, UK) equipped with a He-Ne-laser 4 mW(633 nm).

The morphology and dispersion state of ND-HEMA filled APUA were investigated using a field emission scanning electron microscope (FE-SEM) (JEOL, JSM-6700F) at an accelerating voltage of 10 kV and transmission electron microscopy (TEM, Philips, cm30) at 200 kV. The cured composites were sectioned by a diamond knife with an Ultramicrotome Leica Reichert, OMU-3, Austria. X-ray diffraction analysis (XRD) was used to evaluate the crystallinity of APUA film with a STADI P diffractometer (STOE, Germany). The X-ray source was Cu/K α radiation at a voltage of 40KV, 30mA current with a radiation wavelength of 1.542 Å. Spectra were recorded in the range of Bragg's angle $2\theta=10^\circ$ to 120° at a scanning rate of $0.2^\circ/\text{min}$.

Dynamic mechanical analyses (DMA) were carried out with a Tritec 2000 DMA (Triton, Tritec Technology, England). The scans were performed in a single cantilever bending mode operating under a dry nitrogen purge. The temperature-dependent characterization (storage modulus, loss factor) of each sample was evaluated with a temperature sweep from -100°C to 150°C , at a frequency of 1 Hz, with a heating rate of $4^\circ\text{C}/\text{min}$ and at 0.02% strain. The rectangular specimens with dimensions of $10\text{mm}\times 5\text{mm}\times 1\text{mm}$ were used. The density of the specimens was determined based on Archimedeian principle in water according to ASTM D792 with Mettler Toledo density meter XS104. Mechanical performance of the samples was evaluated by tensile testing on dumbbell shaped specimens at a cross-head speed of 2 mm/min according to ASTM-D638 using HIWA 2126 universal machine (HIWA Engineering Co., Iran). The tensile testing machine was equipped with a 50kgf(490.3 N) load cell with incremental extensometer to measure the strain

precisely. Three to five tensile tests were carried out for each sample to obtain reliable repeatability.

The contact angle measurements were performed using OCA15 plus (data physics instruments, Germany) equipped with a video measuring system for the evaluation of surface hydrophilicity of APUA and its composites with ND-HEMA. The solvent droplet was put on the air-side surface of a film at room temperature. The average of four measurements was reported as water contact angle of each sample. *In vitro* degradation experiments were performed according to ASTM F 1635 (samples were sterilized using UV treatment and then sterilized media were used). Each sample were placed in an individual 50 mL glass vial containing 0.1M PBS (phosphate buffered saline solution) with a $pH = 7.4 \pm 0.2$. Polymers were kept in a 50 rpm shaking incubator at $37^\circ C$ for up to 180 days. At each time interval, samples were removed from the PBS, placed in distilled water for 5 hr to remove buffer salts then dried under vacuum for 2 days at $37^\circ C$, and weighed to determine dry mass. Mass loss of the samples was obtained as follows:

$$\text{Mass loss (\%)} = \left[\frac{m_0 - m_t}{m_0} \right] \times 100 \quad (1)$$

where m_0 is the pre-degraded dry weight of the polymer and m_t is the dry weight of the material after degradation. The result for each group was reported as an average of three replicates.

2.5. *In vitro* biocompatibility

2.5.1. Cell culture

Human osteosarcoma cells line (MG-63) was obtained from National Cell Bank of Iran (The Pasteur Institute of Iran, Tehran). 10^4 cells were cultured in Dulbecco's modified Eagle's medium (DMEM, Gibco, Scotland) with 10% fetal bovine serum (FBS, Sigma-Aldrich, USA) at $37^\circ C$ in a humidified atmosphere with 5% CO_2 . Cellular experiments were performed using

different composites. Cellular attachment, viability and alkaline phosphatase (ALP) activity were studied as described below. For each cellular experiment three replicates were used per composite. Prior to cell seeding, samples were sterilized using UV treatment for 40 min. Moreover, tissue culture polystyrene (TPS) was used as a negative control groups for all tests.

2.5.2 Cell viability

3-(4,5-dimethylthiazol-2-yl)-2,5-diphenyl tetrazolium bromide (MTT) was used in order to evaluate cell's viability.²² Briefly, 10^4 of MG-63 cells were seeded on the specimens within a 96-well plate and were incubated at 37 °C in 5% CO₂ for 1, 5, and 10 days. After removing the medium, 500 µL of MTT was added to each well and incubated for 4 hours at 37 °C in 5% CO₂. The solution was removed and the formed formazan was solubilized with isopropanol for 15 min. Absorbance was read at 570 nm by ELISA reader (BioTek microplate reader, USA).

2.5.3. Cell attachment study

In order to evaluate the cell proliferation and attachment on the surface of fabricated composites, 10^4 MG-63 osteoblast-like cells were added on the surface of the specimens and incubated in DMEM supplemented with 10% FBS at 37 °C for 1, 5 and 10 days. After each time interval, the DMEM was removed completely and the cells were incubated in 500 µL/well Neutral Red (NR) solution for 4 hours. Then, NR solution was replaced with the stain extraction solution (1% glacial acetic acid, 50% ethanol, and 49% distilled water) in order to dissolve deposited particles and was re-incubated in 37 °C for 15 min. The absorbance was measured at 570 nm using ELISA reader.

2.5.4. ALP activity

All stages were identical to the stages mentioned in MTT assay. Briefly, 20 μ L of cell supernatant was added to 1000 μ L of ALP's kit (Pars Azmun, Iran) according to the manufacturer's protocol at 37°C to evaluate the ALP production of osteoblast cells at each time intervals (1, 5, and 10 days), by conversion of p-nitrophenylphosphate to p-nitrophenol. The absorbance was read at 405 nm using a Nano Drop 2000c spectrophotometer, USA.

2.5.5. Cell morphology

For cell morphological observation, 3×10^4 MG-63 osteoblast-like cells were added on the surface of the samples and incubated in DMEM supplemented with 10% FBS at 37 °C for 4 days. Afterward samples were washed three times with PBS. Then they were fixed with Karnovsky (2.5% glutaraldehyde, 4% paraformaldehyde) solution for 90 minutes followed by the dehydration through a graded series of ethanol, vacuum dried and gold coated for scanning electron microscope (SEM) observation.

2.5.6. Statistical analysis

All of the quantitative data were expressed as means \pm standard deviation. Statistical comparisons were performed using Students't-test. P values of less than 0.05 were considered statistically significant.

Results and Discussion

1.2.Functionalization of ND with HEMA

Figure 1 shows FTIR spectra of the pristine ND, oxidized ND (ND-COOH) and ND-HEMA. For pristine ND the bands at 3435 cm^{-1} and 1630 cm^{-1} are attributed to stretching and bending vibrations of O-H of ND surface, respectively. It is suggested that the bands at 3435 cm^{-1} could

appear either from ambient moisture bound to the ND or during the purification of the raw material.¹⁶ Absorption peak at 1766 cm^{-1} is assigned to the C=O group while the band at 1300 cm^{-1} could be attributed to the C–O stretching vibrations of the-COOH groups. ND-COOH has almost similar absorption peaks as pristine ND but with relative increase in peaks intensity at 3435 cm^{-1} and 3573 cm^{-1} due to more –OH group^{16,23} and shift of C=O vibration peak from 1766 cm^{-1} to 1786 cm^{-1} due to conversion of original functional groups like ketones, aldehydes, alcohols and esters to carboxylic acids and cyclic acid anhydrides (-C(=O)-O-(O=C)-).¹⁹ These observations suggest that air oxidized ND contains higher –COOH groups than as-received ND. The increment of carboxylic group content of ND-COOH compared to as-received ND was also examined using Boehm titration (details not given).

As shown in Figure 1, FTIR spectrum of ND-HEMA shows characteristic peaks at 1712 cm^{-1} (C=O) and 1635 cm^{-1} (C=C) which are relevant to HEMA attached on ND surfaces.¹⁶ Presence of HEMA on ND-HEMA was also examined by TGA. As shown in Figure 2a, ND-COOH is thermally stable up to almost 500°C , because it does not show sensible mass losses up to that temperature. However, ND-HEMA exhibits a step mass loss of almost 5 wt% between $200\text{--}400^\circ\text{C}$ suggesting presence of chemically attached HEMA on the surface of ND which is consistent with literature for HEMA grafted carbon nanotube.¹⁶

The size distribution of all three NDs obtained via DLS is shown in Figure 2b. The average hydrodynamic diameter of as-received ND is found to be 66 nm which is higher than the single primary ND particles with average diameter of 5 nm. This suggests that the smallest entity of as-received ND is indeed an aggregate, consisting of tightly bound ND primary particles, which is consistent with previously reported size for ND.²⁴ Functionalized NDs show slightly larger hydrodynamic diameter and little wider size distribution compared to as-received ND. This is consistent with literature reporting on the average size of functionalized NDs,^{4, 24} which could be

attributed to the coverage of outer surface of NDs by the organic groups. Dispersibility of all NDs in acetone and chloroform is compared in Figure 3. It was revealed that the suspension stability of the as-received and oxidized NDs in both solvents were poor while ND-HEMA showed slightly better dispersion stability.²¹

1.3. Morphological study

To examine dispersion state of ND-HEMAs in APUA matrix, SEM micrographs were taken from the cross-section of fractured surface of samples containing 1 wt% and 2wt% ND-HEMA and the results are given in Figure 4a and b. White spots observed in the SEM micrographs may be the ND-HEMA infiltrated by the APUA matrix; however it appears to be hardly possible to compare the dispersion state of ND-HEMA aggregates in the matrix using SEM data. Instead, TEM micrographs provided better information concerning the dispersion state (see Figures. 4c and 4d). As shown in Figure 4c, dispersed entities with the size of 200-400 nm are evidenced in the sample with 1 wt% ND-HEMA. Considering the DLS data shown in Figure 2b, this entity may be the agglomerate of a few aggregates. This information is closely consistent with our previous report²⁶ that ND in nonpolar media (mineral oil) formed single entities of almost 400 nm size. However, for 2 wt% loading, the agglomerate size becomes larger and the partial interconnectivity between the agglomerate is clearly observed (Figure 4d) suggesting that dispersion state becomes worse at 2 wt% loading.

XRD diffraction pattern of pristine polymer and the composites are displayed in Figure 5. APUA exhibits one broad diffraction peak at 2θ of 19° which is attributed to the presence of small size crystallite originating from its soft segment, i.e. PCL.¹⁸ In APUA/ND-HEMA composites the position of this peak remains unchanged while its intensity increases proportionally with the amount of ND-HEMA content in the samples. This could be indicative of increased crystallinity of composites compared to neat APUA film.

A similar increase in crystallinity of the polymer matrix with ND nanoparticle was described in literature as well^{4,27} which was often explained by the nucleating role of ND originated by its affinity with matrix. The crystallinity (X_C) of samples was calculated using the method described by Young and Lovell.^{1,28} Crystallinity of neat APUA was found to be 38% which was completely consistent with DSC data reported in our previous publication.¹⁸ The crystallinity of ND-HEMA filled APUA increased compared to neat APUA as 42.83%, 43.4% and 41.96% for 0.5 wt%, 1 wt% and 2 wt% loadings, respectively, showing a maximum at 1 wt% loading. The relative loss in crystallinity at 2 wt% loading of ND-HEMA may be due to the spatial hindrance caused by closer particle distance or promotion of agglomeration which constrained further growth of crystallite. The small and new peak observed at 2θ of 43.6° for composites was attributed to the (111) plane of diamond as expected for nanocrystalline diamond.²⁹ With the increase of ND-HEMA concentration the intensity of this peak becomes more prominent as well.

Basically, partial phase separation between hard (isocyanate constituent in polymer) and soft (polydiol) segments of PUs is a unique characteristic resulting in a polymer with two-phase morphology in which hard domain of 5-20 nm average diameter³⁰ is distributed uniformly in the soft domain. The extent of phase separation of hard and soft domains is often described by the degree of phase separation (DPS) which is mostly determined using the FTIR spectrum by measuring the hydrogen bonding index (R),^{31,32} i.e. area ratio between the peak intensity of free-of-hydrogen bonding carbonyl (1730 cm^{-1}) to hydrogen-bonded carbonyl (1702 cm^{-1}), as $DPS=R/R+1$.^{31,32}

FTIR spectrum of APUA and APUA composites was first determined (Figure 6a) and then the corresponding peak for carbonyl groups was deconvoluted to five Gaussian peaks using Origin software (Figure 6 b). As given in Table 1, DPS of pristine APUA is increased by incorporation of ND-HEMA demonstrating its capability in formation of further hard domains. Consistent with

crystallinity, there is a maximum DPS at 1 wt% loading of ND-HEMA suggesting that the agglomeration prevents the formation of further separated hard domains possibly due to the spatial hindrance.

1.4. Mechanical and dynamic mechanical properties

Dynamic mechanical properties of APUA/ND-HEMA composites are shown in Figure 7. $\tan\delta$ -temperature curve (Figure 7a) exhibits multiple transition peaks for both neat APUA and the composites suggesting multiphase morphology of the matrix which basically includes soft and hard domains. According to Alishiri et al,¹⁸ the prominent broad peak observed between -60 °C to -10 °C is attributed to glass-rubber transition of soft domain, i.e. PCL, of neat APUA. There is also very minor peak in $\tan\delta$ -temperature curve almost at 10 °C (see vertical dashed line position in Figure 7a) which could be attributed to relaxation behavior of soft domain as well. Such heterogenous relaxation behavior of amorphous region of soft domain in neat APUA is more likely induced by crystalline region of soft domain and the influence of dispersed hard domain on the amorphous region. Accordingly, the amorphous regions close to crystalline and hard domains have more likely restricted molecular mobility.

As shown in Figure 7b, a stepwise loss in storage modulus of neat APUA is observed at temperatures corresponding with prominent glass-rubber transition peak in $\tan\delta$ curve. However, there is no distinct storage modulus step loss for the minor relaxation peak, as mentioned by $\tan\delta$ curve, probably due to overlapping with that of prominent transition $\tan\delta$ peak observed below -10 °C. Accordingly, glass-rubber transition temperature of soft domain (referred to as $T_{g,S}$) was obtained using the storage modulus-temperature curve by intersecting two tangents; one below transition loss and the other near inflection point of the modulus transition loss according to ASTM-E1640. As a result, $T_{g,S}$ of neat APUA was found to be -58.5 °C (see Table 1). According

to Figure 7b, as storage modulus of APUA exhibits a significant stepwise drop around $T_{g,S}$ (see Figure 7b), it can be deduced that the soft domain forms the continuous phase in which the hard domains are distributed uniformly as dispersed phase.³³

As reported in Table 1, incorporation of ND-HEMA into APUA increases $T_{g,S}$ slightly, however, it influences greatly the $\tan\delta$ peak of neat APUA at 10 °C. Accordingly, the minor relaxation peak of neat APUA becomes larger and shifted to higher temperatures in presence of ND-HEMA (see Figure 7a). This behavior could be attributed to the increment of DPS and crystallinity in presence of nanodiamonds, as well as presence of nanodiamonds itself in soft domain inducing more heterogeneity in relaxation behavior of amorphous region.

As deduced in Figure 7, the small $\tan\delta$ peak around 45 °C which is correspondent with a step loss in storage modulus of APUA, is indeed related to the glass transition of hard phase (crosslinked acrylate/isocyanate containing domain), while a small sharp peak observed around 60 °C indicates the melting point (T_m) of crystalline phase, as discussed by Alishiri et al.¹⁸ Glass transition temperature of hard domain (denoted by $T_{g,H}$) was obtained using the storage modulus data as well. As reported in Table 1, addition of ND-HEMA to APUA results in the enhancement of $T_{g,H}$ which could be due to the interaction of hard domain with the ND-HEMA probably via the chemical bonding through the HEMA functional groups involved in the crosslinking reaction.

DMA data suggest that ND-HEMA is interacted by both hard and soft domains of APUA. According to literature,^{30,33-34} average diameter of dispersed hard domain ranges between 5- 20 nm with a hard inter-domain distances within 5-25 nm which are much smaller than the ND-HEMA aggregate size obtained from DLS and TEM. Such morphological feature led us to assume that ND-HEMA is preferentially localized at soft continuous domain, however, there should be possibility for dispersed hard domains (due to its nano-scale size) to attach on the outer

surface of ND-HEMA aggregates periodically (not like a uniform layer at outer surface). Somewhat similar morphological model was suggested by Fernández-d'Arlas et al. for thermoplastic PU/carbon nanotube composites.³⁵ Presence of HEMA functional group on outer surface of ND-HEMA and in APUA structure provides a tendency for attachment of hard domain on the outer surface of ND-HEMA by involving in crosslinking reaction.

Storage modulus of APUA was observed to enhance with incorporation of ND-HEMA particles, indicating reinforcement effect of ND-HEMA on APUA.¹⁷ According to Figure 7b, the extent of improvement in storage modulus is much higher below $T_{g,s}$, where the soft domain stays in its glassy state, suggesting ND-HEMAs interact mainly with APUA soft domain.^{37,38} Higher storage modulus of ND-HEMA filled APUA is attributed to restricted mobility of polymer chains due to interfacial bonding between nanodiamonds and APUA matrix,³⁹ restricting composite ability to deform by strengthening APUA molecules.⁴⁰ The extent of enhancement in storage modulus is found to be dependent on the ND-HEMA content. APUA composite with 1 wt% ND-HEMA particles exhibits the highest improvement in storage modulus, while at 2 wt% loading a relative decrease is observed which is more likely due to the agglomeration of ND-HEMA in APUA.⁴¹

As shown in Figure 8a, incorporation of ND-HEMA enhances the tensile properties of APUA significantly, e.g. 175% in elastic modulus and 40% in tensile strength at 1 wt% loading. Such significant improvements in tensile properties of bone implantable PU are much higher than other reinforcements reported in literature like β -TCP (maximum improvement 15% for compressive modulus and 5 % for compressive strength at 10wt% β -TCP¹) and nHA (maximum 17 and 20 % improvements in the young modulus and tensile strength, respectively, at 10 wt% loading⁴²).

The effectiveness of ND-HEMA in tensile properties of APUA can be attributed to the strong interfacial interaction between polymer-filler and uniform dispersion of ND-HEMA within the matrix.⁴³ Surface functional group of ND-HEMA is effective in fine dispersion in the matrix and achievement of good interfacial interaction in the composite. Furthermore, enhancement in mechanical properties can be attributed partly to the increase of crystallinity of APUA matrix in presence of ND-HEMA^{13,44} and increment in DPS.³¹⁻³² Crystalline structure has stronger mechanical properties³⁸ and can contribute significantly on overall mechanical properties of semi-crystalline polymers. It is noteworthy that localization of ND-HEMA in soft domain, as discussed above, provides unique opportunity to enhance the mechanical properties of mechanically weaker phase of APUA, because, the hard domain is rigid and fully crosslinked phase¹⁸ with higher mechanical properties acting as rigid filler itself in APUA matrix. The relative decrease in mechanical properties of 2 wt% loading ND-HEMA is completely in line with crystallinity and DPS data as well which is more likely related to the loss in degree of dispersion of ND-HEMA at this concentration. Fracture energy was also calculated from the area under the stress-strain curves, see Figure 8b. Addition of ND-HEMA causes a decrease in fracture energy of APUA, as expected, however APUA/ND-HEMA(1 wt%) shows the largest fracture energy amongst the composites, probably due to its unique morphological feature, i.e. higher DPS and crystallinity with almost fine ND dispersion.

3.4. Effect of ND-HEMA on surface properties and biodegradability of APUA

Wetability of a synthetic specimen provides important information concerning its biocompatibility and surface hydrophilicity.⁴⁵ Indeed, surface hydrophilicity of a polymer film is very important for homogeneous and sufficient cell seeding and growth.⁴⁶ The surface hydrophilicity of samples was characterized using water contact angle measurements, as shown in Figure 9. It is interesting to note that presence of ND-HEMA in APUA decreased the contact

angle of APUA and therefore improved the hydrophilicity of APUA film. This can be due to hydrophilic nature of both ND⁴⁷ and HEMA.⁴⁸ Such improvement in hydrophilicity is particularly desirable in biomedical applications of APUA/ND-HEMA composites. According to Figure 9a, a relative increase in water contact angle of APUA/ND-HEMA (2wt %) suggests agglomeration of nanoparticles which made them slightly more hydrophobic. It is to be noted that the water contact angle of the composites obtained in this study is lower than the commercial implantable devices (75-80°)⁴⁹ and PU based biocompatible composites, for instance PU/bioglass composites (69-74°).⁵⁰

To investigate the role of ND-HEMA on hydrolytically degradation rate, *in vitro* degradation test method used in surgical implants was utilized. Figure 9b shows the mass remaining profile of neat APUA and APUA/ND-HEMA composites versus incubation time in PBS over 6 months. It was expected that the sample would undergo hydrolysis degradation through the ester bonds of PCL.⁵¹ It is observed that all samples shows mass loss with time indicating their biodegradation. Interestingly, ND-HEMA has increased the degradability of APUA so the difference between mass loss of neat APUA and APUA/ND-HEMA becomes much prominent at longer times suggesting the positive role of ND-HEMA on acceleration of hydrolytic degradation of APUA. Such behavior can be ascribed to hydrophilic nature of ND-HEMA enhancing the water absorption that would improve the rate of hydrolysis of PCL ester bonds.⁵² Consistent with mechanical properties and water contact angle data, the biodegradation is dependent on ND-HEMA content so a relative loss in biodegradation is observed for 2 wt% loading possibly due to its poor dispersion.

The degradation property is suitable in tissue engineering for the bone repair.⁵³ It is necessary that the degradation rate of composites should tailor the healing rate of bone. In this way the initial weight loss of composites during the first days should be low as bone is defected,⁵⁴ and in the

course of regeneration of bone tissue, the bone substitute should be degraded in line with the bone reconstruction rate.⁵⁵ It is to be noted that many biodegradable bone substitutes reported in literature^{1, 51} showed low degradation rate, therefore any acceleration is indeed desirable.

3.5. *In vitro* biocompatibility

The biocompatibility of the neat APUA and its composites was assessed through *in vitro* cell culture experiments. Literature shows that there is a major concern regarding the toxicity of PUs and their biodegradation products.^{52,56} This is particularly true for PUs derived from aromatic diisocyanates that can be biodegraded into toxic products composed of aromatic diamines. Therefore, APUA produced in this work was based on aliphatic diisocyanates whose nontoxic effects were evaluated by Rodrigues et al.⁵² via measuring their effects on the viability of retinal cells.

The potential toxicity of carbon nanoparticles reported in literature has shown a great deal of controversy and confusion. Several authors have reported favorable cellular interactions with carbon nanoparticles,⁵⁷⁻⁵⁸ while some others have reported decreased cell viability.⁵⁹⁻⁶⁰ The controversy may be originated from a number of variables used in their studies including cell type, nano particle type (MWNT, SSWNT, ND, CNF), shapes and size, surface chemistry, level of impurities as well as local concentration and surface functionalization. Schrand et al.⁶¹ reported that ND is less cytotoxic than other carbon materials. Moreover, several *in vitro* experiments with different cell lines generally showed no or very little toxicity of all tested NDs.⁶² However, there may be the situations in which NDs can exhibit certain cytotoxic effects as reported by Burleson.⁶² Nevertheless, according to open literature,^{4,63} the ND powder itself up to the concentration of 1000µg/ml did not produce significant changes in the viability of neuroblastoma, kidney, 7F2 osteoblasts and epithelial cells. Therefore, it is imperative to investigate the toxicity

and biocompatibility of ND-based biomaterials before they can be considered for widespread acceptance and use. As APUA/ND-HEMA composite is targeted to be introduced as potential material for bone applications, comprehensive understanding about toxicity and biocompatibility of this composite is crucial requirement.

The cells viability next to APUA and three different fabricated composites (0.5, 1 and 2 wt% loadings) on MG-63 cell line were quantified by MTT assay as shown in Figure10a. It is to be noted that the carcinoma cell line is normally used in biocompatibility studies because of its rapid rate of growth and proliferation along with easy separation through the viability test compared to normal cell line. According to the MTT assay, exposure of the cells to neat APUA and APUA/ND-HEMA composites did not influence cell viability in a significant manner compared to the control group (TPS). According to Figure10a, viable cells for all samples are more than 80% that stands within acceptable biocompatibility range, because a material is considered to be cytotoxic when its viable cells becomes less than 70%.⁶⁴ Nevertheless, the attached cells were well spread on APUA and APUA/ND-HEMA composites suggesting their unaffected cell functions. The results indicate that in presence of NDs, the cells still survive and grow well which is in line with literature data.⁴ Actually, Burleson et al.⁶² reported that the effect of NDs on carcinoma cell line was more pronounced than on normal human cells.

It is found that viability of MG-63 cells for APUA/ND-HEMA is slightly lower than that of neat APUA, but the difference is not considerable. Also consistent with literature data,⁴⁶ the result suggested that the hydrophilic surface of the lower content of ND-HEMA in composites was more favorable for the cell spreading and growth than the hydrophobic surface of the higher content films. It could be observed that cytotoxicity of all samples shows a slight reduction at 5th day but at longer incubation time of 10th day inverse result is obtained (with $p > 0.05$ which is statistically insignificant). The obtained results demonstrated that there was not any significant

difference in the cell viability and the overall cell morphology of the samples during the incubation period.

The number of cells adhered to the samples is shown in Figure 10b. No clear differences are observed in MG-63 cell attachment of APUA/ND-HEMA composites with increasing ND content in the first day. The lack of clearly distinguishable effect may be because of negligible difference in their wettability (water contact angle) which is believed to cause significant changes in cell adsorption during the 24h cell culture incubation period. Furthermore, the carcinogenic cell-type used (MG-63) may have been less sensitive to wetting conditions than primary cells.⁶ Similar to some studies⁶⁵ no correlations between chemical composition and cell attachment were observed. An increase in the total osteoblast number was found with increasing culture incubation period (from 5th to 10th day) in all samples (Figure 10b).

The effect of ND-HEMA on MG-63 osteoblast differentiation of APUA was further analyzed by ALP activity, since ALP is regarded to be an important phenotype of bone-forming cells.⁴ The ALP gene's expression levels in MG-63 cells cultured at three different times (1st, 5th and 10th days) on neat APUA and its composite with ND-HEMA were evaluated and the results were compared to those in MG-63 cells cultured on TPS for similar periods. According to Figure 10c, no considerable ALP is produced by seeding the MG-63 cells on all films in comparison with TPS. The incorporation of ND-HEMA into the films did not cause any significant differences in ALP production by MG-63 cells in 1st and 10th days compared with neat APUA polymer. ALP activity was found in all samples to be time-dependent. When comparing the data at 5th and 10th days to those at 1st day, we found a significant decrease in ALP gene expression ($p < 0.05$). Other osteogenic cell lines, such as murine osteoblast (7F2) cells on PLLA/ND nanocomposites also exhibited a similar inverse relationship between incubation time and ALP gene expression *in vitro*.⁴

Results of osteoblast developmental stages indicated that production of ALP decreased as the proliferation was speeded up. Therefore, an inverse relationship between growth and ALP production were obtained. Similar results were reported in previous *in vitro* investigations for many cell types, e.g. osteoblast-like cell lines (MC3T3-E1).⁶⁶

Overall, the data from ALP assay as well as MTT assay suggest that APUA composites containing up to 2 wt% ND-HEMA are non-cytotoxic, support MG-63 cell proliferation and osteogenic differentiation, and therefore can be used for biomedical applications. Furthermore the results indicated that the incorporation of ND-HEMA in the samples had no adverse effect on the proliferation, ALP production and osteoblast attachment in comparison with neat APUA.

In order to assess the morphology and cytoskeletal architecture of MG-63 cells on APUA and APUA/ND-HEMA composites, the cells were fixed after 4 days post-seeding. SEM micrographs (Figure 10d) show proliferation and attachment of cells on to the films. SEM microphotographs of cells grown on samples suggested that the proliferation of cells could maintain their normal morphology while adhered on the surface of films. Therefore SEM results confirmed that MG-63 cells have become fully confluent on all samples. Moreover, the *in vitro* appearance of the cells was consistent with that reported in literature.

Conclusion

In this study, in situ polymerized APUA/ND-HEMA composites at low concentrations, i.e. 0.5 to 2 wt%, were synthesized and their mechanical and biocompatibility characterized experimentally. Morphological investigation showed fine distribution of ND-HEMA aggregates within APUA matrix, however, larger agglomerates were observed at higher concentrations, i.e. 2wt%. Enhancement in crystallinity of the composites was corroborated by XRD. Moreover, it was found that ND-HEMA was localized in soft domain of APUA providing opportunity to

strengthen mechanically weaker phase of APUA. Mechanical analysis showed a significant improvement in mechanical properties, e.g. 175% in elastic modulus and 40% in tensile strength, at 1 wt% loading of ND-HEMA, which were much higher than other reinforcements reported in literature, such as β -TCP or nano HA, in PU based composites for biomedical applications. Appropriate interfacial interaction between APUA and ND-HEMA, increment in crystallinity and DPS were found to be influential parameters for such enhancement in mechanical properties. Cytotoxicity evaluation of the composites using human osteosarcoma cells (MG-63 cell line) showed no adverse effect on biocompatibility. Results of osteoblast developmental stages indicated an inverse relationship between proliferation and production of ALP. The present investigation showed that ND-HEMA can be promising nanoparticle which is able to enhance the mechanical properties without destructive role on the biocompatibility of APUA. This makes the APUA/ND-HEMA favorable biomaterial for hard tissue engineering where the enhanced mechanical properties are required.

Acknowledgment

This work was financially supported by Iran National Science Foundation (INSF). The authors gratefully acknowledge their support.

References

- 1 R. Adhikari, P.A. Gunatillake, I. Griffiths, L. Tatai, M. Wickramaratna, S. Houshyar, T. Moore, R.T. Mayadunne, J. Field, M. McGeed, T. Carbone, *Biomaterials*. 2008, **29**, 3762-3770.
- 2 J.E. Dumas, T. Davis, G.E. Holt, T. Yoshii, D.S. Perrien, J.S. Nyman, T. Boyce, *Acta Biomater*. 2010, **6**, 2394-2406.

- 3 I.H. Pereira, E. Ayres, P.S. Trício, A.M. Góes, V.S. Gomidea, E.P. Junior, R.L. Oréface, *Acta Biomater.* 2010,**6**,3056-3066.
- 4 Q. Zhang, V.N. Mochalin, I. Neitzel, I.Y. Knoked, J. Han, C.A. Klug, J.G. Zhou, P.I. Lelkes, Y. Gogotsi, *Biomaterials.* 2011,**32**,87-94.
- 5 X. Chen, J.Wang, J. Zou, X. Wu, X. Chen X, F. Xue, *J. Appl. Polym. Sci.*2009, **114**, 3407-3413.
- 6 R. Verdejo, G. Jell, L. Safinia, A. Bismarck, M.M. Stevens, M.S.P. Shaffer, *J. Biomed. Mater. Res. Part A.*2009,**88**,65-73.
- 7 H. Deka, N. Karak. R.D. Kalita, A.K. Buragohain, *Carbon.* 2010, **48**,1-10.
- 8 C. Zhao, W. Zhang, *Eur. Polym. J.*2008,**44**,1988-1995.
- 9 V.N. Mochalin, O. Shenderova, D. Ho, Y. Gogotsi, *Nat. Nanotechnol.*2012,**7**,11-23.
- 10 V. Bershtein, L. Karabanova, T. Sukhanova, P. Yakushev, L. Egorova, E. Lutsyk, A. Svyatyna, M. Vylegzhanina, *Polymer.* 2008,**49**,836-842.
- 11 L. Grausova, A. Kromka, L. Bacakova, S. Potocky, M. Vanecek, V. Lisa, *Diam. Relat. Mater.* 2008, **17**,1405-1409.
- 12 V.N. Khabashesku, J.L. Margrave, E.V. Barrera. *Diam. Relat. Mater.*2005,**14**,859-866.
- 13 S. Morimune, M. Kotera, T. Nishino, K. Goto, K. Hata, *Macromolecules.* 2011,**44**, 4415-4421.
- 14 I. Neitzel, V. Mochalin, I. Knoke, G.R. Palmese, Y. Gogotsi, *Compos. Sci. Technol.* 2011,**71**,710-716.
- 15 A.P. Voznyakovskii, B.M. Ginzburg, D. Rashidov, D.G. Tochil, S. Tuichiev, *Polym. Sci. Ser. A.* 2010,**52**,1044-1050.
- 16 N.A. Kumar, H.S. Ganapathy, J.S. Kim, Y.S. Jeong, Y.T. Jeong, *Eur. Polym. J.*2008,**44**,579-586.

- 17 P. Protopapa, E. Kontonasi, D. Bikiaris, K.M. Paraskevopoulos, P. Koidis, *Dental. Mat. J.* 2011,**30**,222-231.
- 18 M. Alishiri, A. Shojaei, M.J. Abdekhodaie, H. Yeganeh, *Mater.Sci.En., C* . 2014,**42**,763-773.
- 19 C. Li, C.L. Huang, *Colloids.Surf. A.*2010,**353**,52-56.
- 20 L. Li, J.L. Davidson, C.M. Lukehart, *Carbon.* 2006,**44**,2308-2315.
- 21 A. Krueger, T. Boedeker, *Diam. Relat Mater.*2008,**17**,1367-1370.
- 22 M. Zanetta, N. Quirici, F. Demarosi, M.C. Tanzi, L. Rimondini, S. Fare, *Acta Biomater.*2009,**5**,1126-1136.
- 23 S. Ji, T. Jiang, K. Xu, S. Li, *Appl. Surf. Sci.*1998,**133**,231-238.
- 24 X. Zhang, M. Chen, R. Lam, X. Xu, E. Osawa, D. Ho. *ACS Nano*, 2009,**3**(9),2609-2616.
- 25 Q. Zhang, V.N. Mochalin, I. Neitzel, I.Y. Knoke, J. Han, C. Klug. A, Zhou J. G, Lelkes P.I, Gogtsi Y, *Biomaterials.* 2011,**32**,87-94.
- 26 N.A. Burns, M.A. Naclerio, S.A. Khan, A. Shojaei, S.R. Raghavan, *J. Rheol.* 2014,**58**, 1599-1614.
- 27 U. Maitra, K.E. Prasad, U. Ramamurty, C.N. Rao, *Solid State Commun.*2009,**149**,1693-1697.
- 28 R. Young, P. Lovell. *Introduction to Polymers.*2nd. London, Chapman & Hal, 1991.
- 29 Q. Zou, Y.G. Li, L.H. Zou, M.Z. Wang, *Mater. Charact.*2009,**60**,1257-1262.
- 30 B.F. Arlas, L. Rueda, R. Fernández, U. Khan, J.N. Coleman, I. Mondragon, A. Eceiza, *Soft Matter.*2010,**9**,79-93.
- 31 M. Aurilia, F. Piscitelli, L. Sorrentino, M. Lavorgna, S. Iannace, *Eur. Polym. J.* 2011,**47**(5), 925-936.
- 32 H. Xia, M. Song, *Soft Matter.*2005,**1**,386-394.
- 33 Z.S. Petrovi, D. Hong, I. Javni, N. Erina, F. Zhang, J. Ilavský, *Polymer.* 2013,**54**,372-380.
- 34 R.G. Heijkants, L.W. Schwab, R.V. Calck, J.H. Groot, A.J. Penning, A.J. Schouten, *Polymer.*2005,**46**,8981-8989.

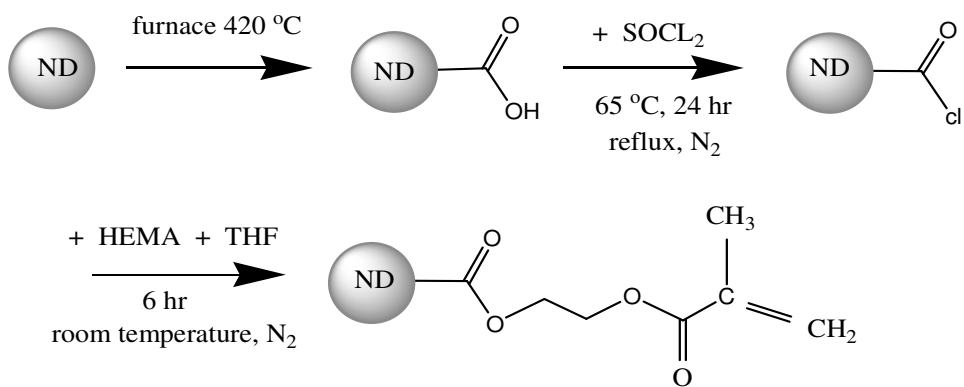
- 35 B.F. Arlas, U. Khan, L. Rueda, N. Coleman, I. Mondragon, M.A. Corcuera, A. Eceiza, *Compos. Sci. Technol.* 2011, **71**, 1030-1038.
- 36 S. Razavi, A. Shojaei, R. Bagheri, *Polym. Adv. Technol.* 2011, **22**, 690-702.
- 37 A.F. Osman, G.A Edwards, T.L. Schiller, Y. Andriani, K.S. Jack, I.C. Morrow, P.J. Halley, D.J. Martin, *Macromolecules* 2012, **45**, 198-210.
- 38 B.F. Arlas, U. Khan, L. Rueda, L. Martin, J.A. Ramos, J.N. Coleman, M.L. González, A. Valea, I. Mondragon, M.A. Corcuera, *Compos. Sci. Technol.* 2012, **72**, 235-242.
- 39 M. Raja, A.M. Shanmugaraj, S. Hun, J. Subha, *Mater. Chem. Phys.* 2011, **129**, 925-931.
- 40 S.A. Rakha, R. Raza, A. Munir, *Polym. Compos.* 2013, **34**, 811-818.
- 41 J. Deng, J. Cao, J. Li, H. Tan, Q. Zhang, Q. Fu, *J. Appl. Polym. Sci.* 2008, **108**, 2023-2028.
- 42 A.B. Valencia, G.C. Torre, A.D. Moller, H.E. Ponce, E. Medina, *Int. J. Phys. Sci.* 2011, **6**, 6681-6691.
- 43 Y. Zhai, Z. Wang, W. Huang, J.J. Huang, Y.Y. Wang, Y.Q. Zhao, *J. Mater. Sci. Eng. A.* 2011, **528**, 7295-7300.
- 44 K.E. Prasad, B. Das, U. Maitra, U. Ramamurty, C.N. Rao, *PNAS*. 2009, **106**, 13186-13189.
- 45 G.A. Abraham, A.A. Queiroz, J.C. Roman, *Biomaterials.* 2002, **23**, 1625-1638.
- 46 H. Ryeon, H.S. Baek, M.H. Lee, Y.I. Woo, D.W. Han, M.H. Han, H.K. Baik, W.S. Choi, K.D. Park, K.H. Chung, J.C. Park, *Surf. Coat. Technol.* 2008, **202**, 5768-5772.
- 47 A.M. Schrand, S.A. Hens, O.A. Shenderova, *Crit. Rev. Solid. State. Mater. Sci.* 2009, **34**, 18-74.
- 48 A. Ghaffar, P.G. Verschuren, J.A. Geenevasen, T. Handels, J. Berard, B. Plum, A.A. Dias, P.J. Schoenmakers, S.V. Wal, *J. Chromatogr. A.* 2011, **1218**, 449-458.
- 49 K. Gorna, S. Gogolewski. *Polym. Degrad. Stab.* 2003, **49**, 475-485.

- 50 J.L. Ryszkowska, M. Auguscik, A. Sheikh, A.R. Boccaccini, *Compos. Sci. Technol.* 2010,**70**,1894-1908.
- 51 S. Mondal, D. Martin. *Polym. Degrad. Stab.*2012,**97**,1553-1561.
- 52 G. Rodrigues, S. Jr, F .Behar-cohen, E. Ayres, R.L. Oréfice. *Polym. Degrad. Stab.*2010,**95**,491-499.
- 53 Z. Dong Z, Y. Li, Q. Zou, *Appl. Surf. Sci.*2009,**255**,6087-6091.
- 54 E. Orava, J. Korventausta, M. Rosenberg, M. Jokinen, A. Rosling, *Polym. Degrad. Stab.*2007,**92**,14-23.
- 55 A.J. Aho, T. Tirri, J. Kukkonen, N. Strandberg, J. Rich, J. Seppala, A.Y. Urpo, *J. Mater. Sci. Mater. Med.*2004,**15**,1165-1173.
- 56 J.P. Santerre, K. Woodhouse, G. Laroche, R.S. Labow, *Biomaterials.* 2005,**26**,7457-7470.
- 57 J. Meng, H. Kong, H.Y. Xu,L. Song, C.Y. Wang, S.S. Xie, *J. Biomed. Mater. Res. Part A.* 2005,**74**,208-214.
- 58 P.R. Supronowicz, P.M. Ajayan, K.R. Ullmann,B.P.Arulanandam, D.W. Metzger, R. Bizios, *J. Biomed. Mater. Res.* 2002,**59**,499-506.
- 59 F . Tian, D .Cui, H. Schward, G . Estrada, H . Kobayashi, *Toxicol in Vitro.* 2006,**20**,1202-1212.
- 60 J.L .Mckenzie, M.C. Waid, R. Shi, T.J. Webster, *Biomaterials.* 2004,**25**,1309-1317.
- 61 A.M. Schrand, J. Johnson, L.M. Dai, M. Hussain, J. J. Schlager, L. Zhu, Y. Hong, E . Osawa, In, Webster TJ, editor.Safety of nanoparticles.From manufacturing to medical applications. New York, Springer,2009,pp. 159.
- 62 T. Burlison, N. Yusuf, A. Stanishevsky, *J. Achivement Mater. Manufac. Eng.* 2009,**37**,258-263.

- 63 A.M. Schrand, L. Dai, J.J. Schlager, S.M. Hussain, E. Osawa, *Diam. Relat. Mater.* 2007,**16**,2118-2123.
- 64 J.M. Page, E.M. Prieto, J.E. Dumas, K.J.Zienkiewicz , J.C . Wenke, P.B. Baer, S.A. Guelcher, *Acta Biomater.* 2012,**8**, 4405-4416.
- 65 S. Guelcher, A. Srinivasan, A .Hafeman, K. Gallagher, J. Doctor, S. Khetan, S. Mcbride, S. Hollinger J. *Tissue Eng.* 2007,**13**,2321-2333.
- 66 B. Saad, Y. Kuboki, M. Welti, G.K.Uhlschmid, P.Neuenschwander, U.W. Suter, *Artif. Organs.* 2000,**24**,939-945.

Table 1–Density, morphological and thermal transition data of samples.

Sample	R	DPS	ρ (g/cm ³)	T _{g,s} (°C)	T _{g,H} (°C)
APUA	0.97	0.49	1.161	-58.5	39.8
APUA/ND-HEMA (0.5 wt%)	1.41	0.58	1.171	-58	46.9
APUA ND-HEMA (1 wt%)	1.63	0.62	1.174	-56.4	48
A UA/ND-HEMA (2 wt%)	1.36	0.57	1.171	-55.5	46.5



Scheme 1- Reaction schemes for preparation of ND-HEMA.

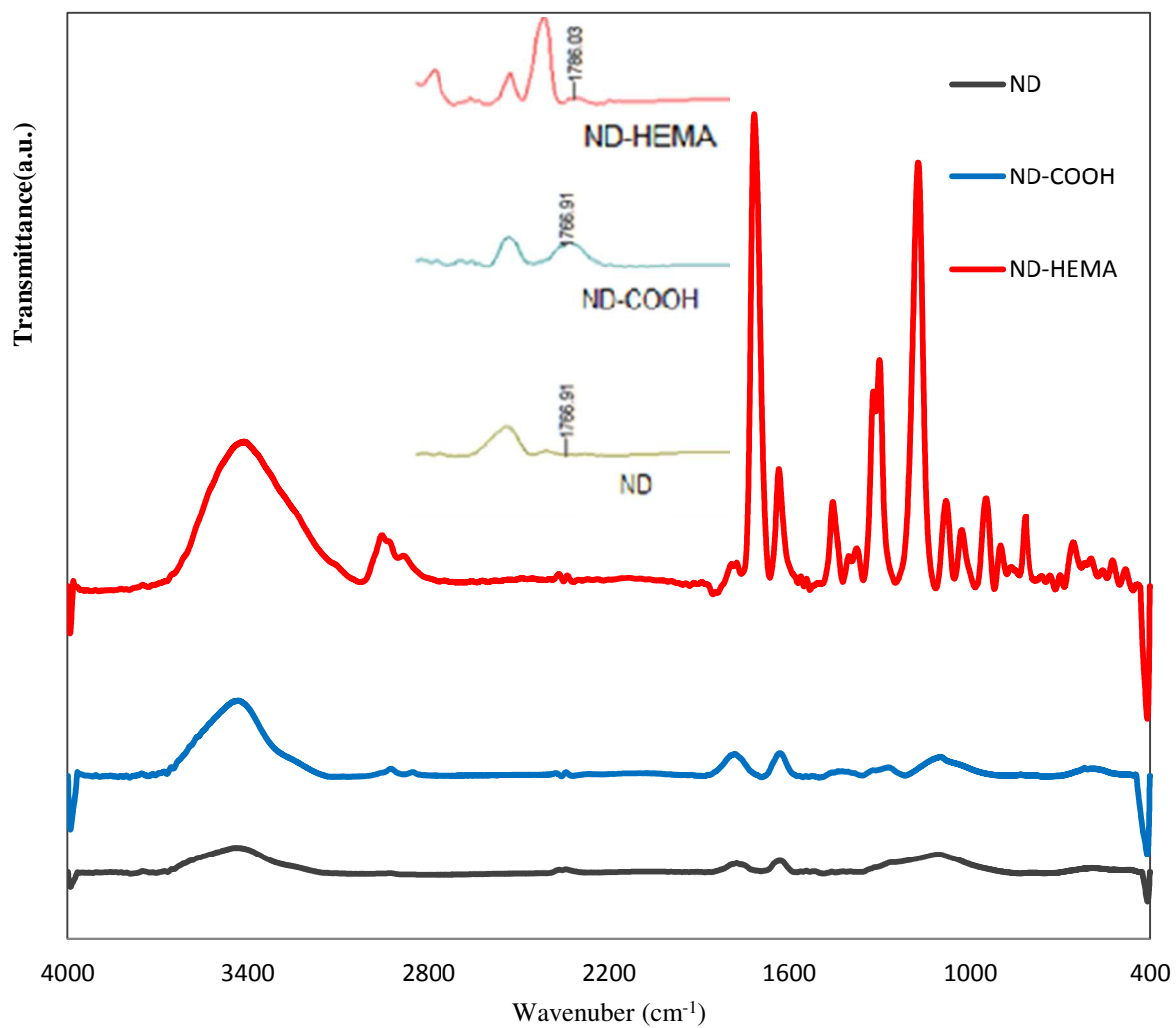


Fig. 1. FTIR spectra of ND, ND-COOH and ND-HEMA

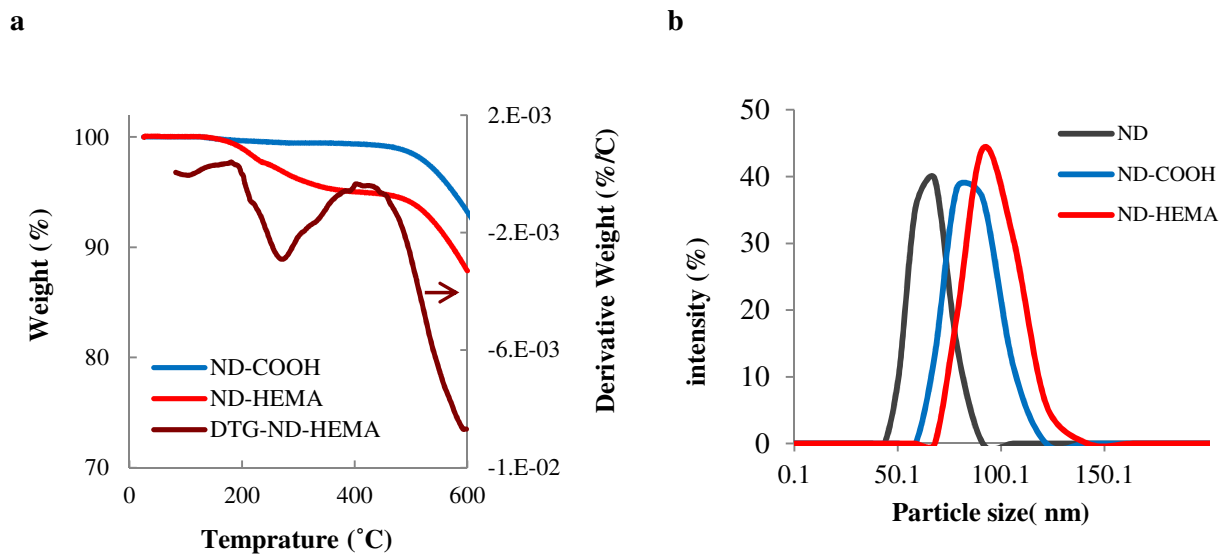


Fig 2. a) TGA and DTG thermograms of functionalized ND particles , b) particle size distribution of as-received ND and functionalized NDs.

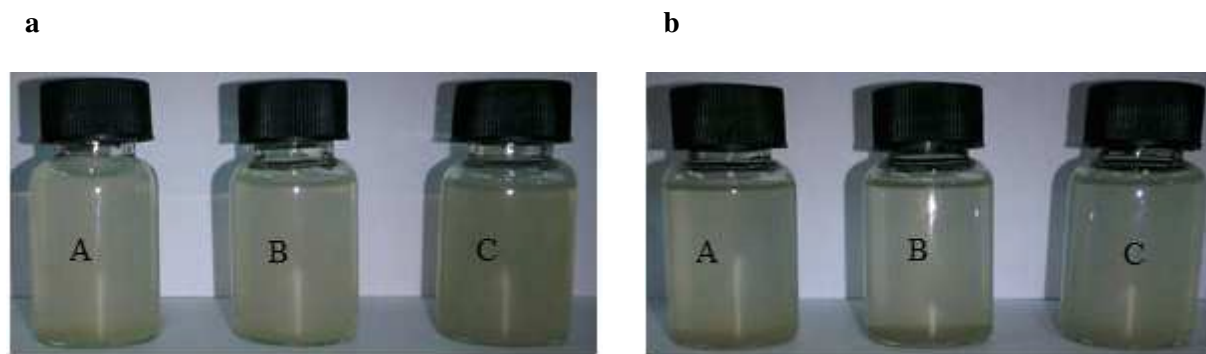


Fig. 3. Dispersibility of the NDs; (A) pristine NDs, (B) ND-COOH, (C) ND-HEMA ; in a) acetone, b) chloroform after 1hr. 5mg of the NDs were suspended in 15 ml of the solvents and then sonicated for 3 min via bath type sonicator.

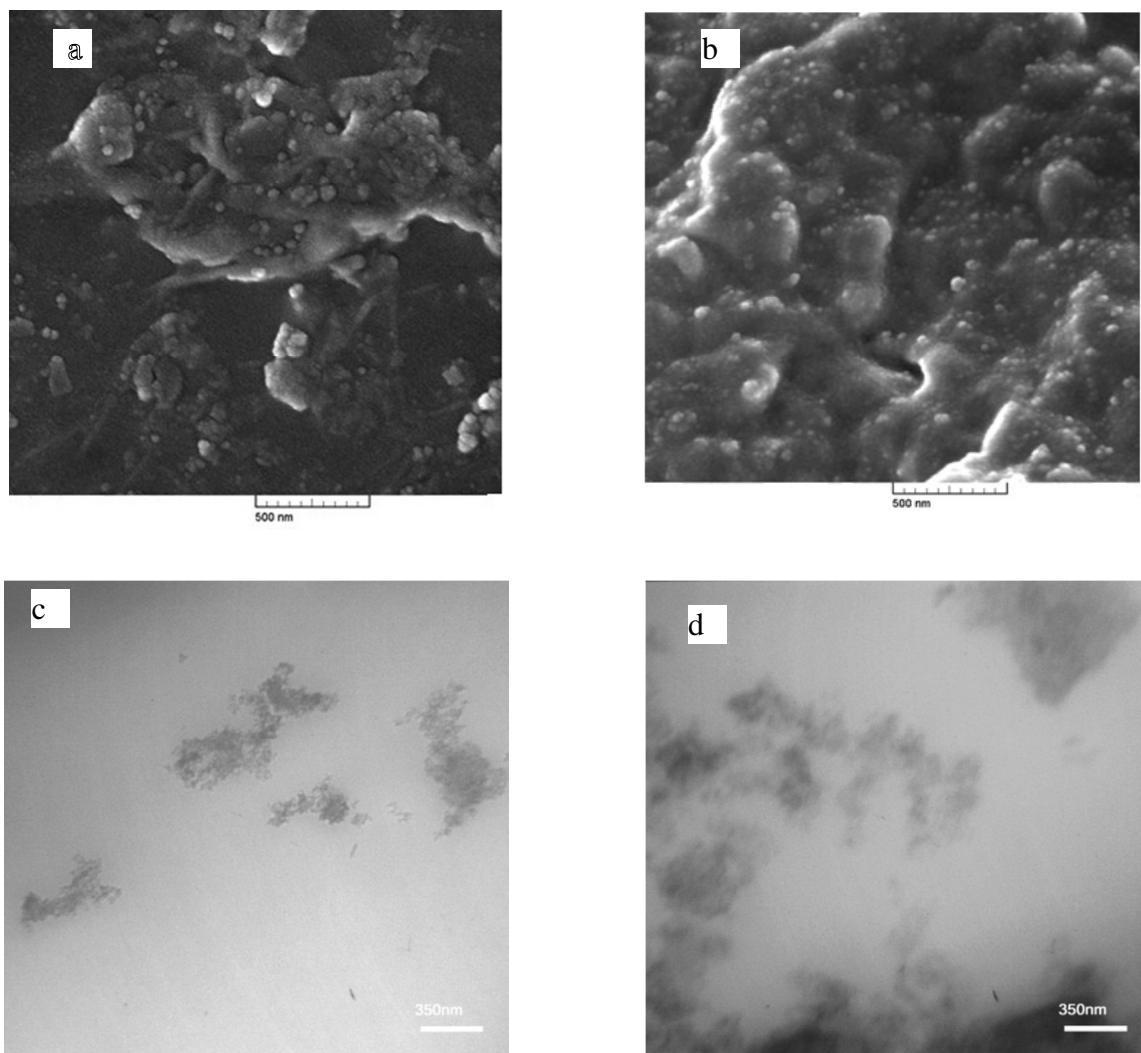


Fig.4. Micrographs of APUA/ND-HEMA a) FESEM of 1wt% ND-HEMA, and b) FESEM of 2wt% ND-HEMA, c) TEM of 1wt% ND-HEMA, and d) TEM of 2wt% ND-HEMA.

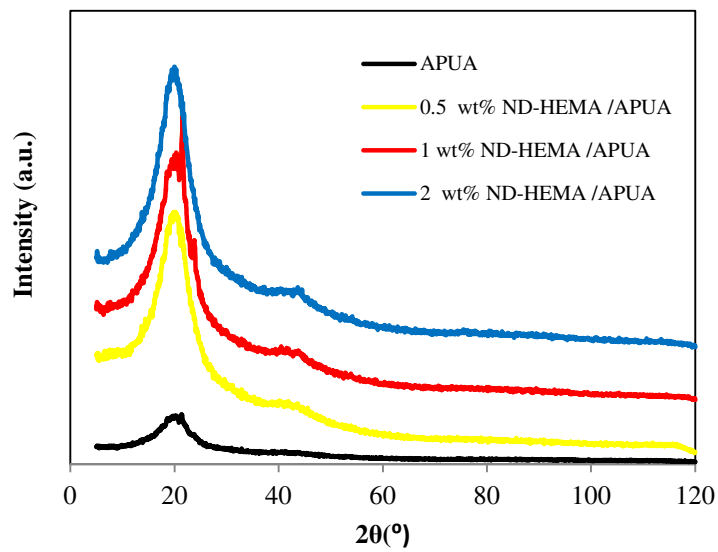


Fig. 5. XRD pattern of neat APUA and its composites with ND-HEMA.

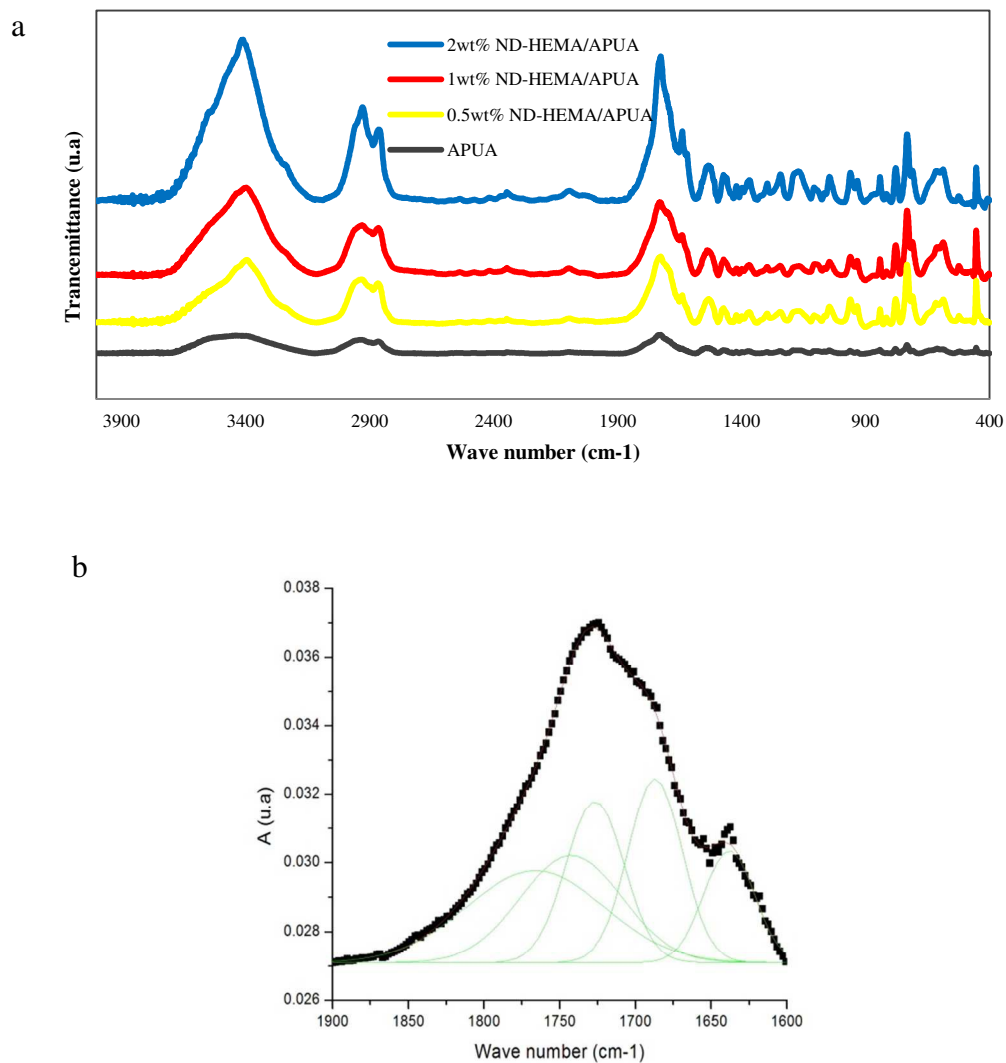


Fig. 6. a) FTIR spectra of APUA nanocomposites, b) deconvoluted FTIR spectra in the carbonyl stretching region of APUA/ND-HEMA (1 wt%).

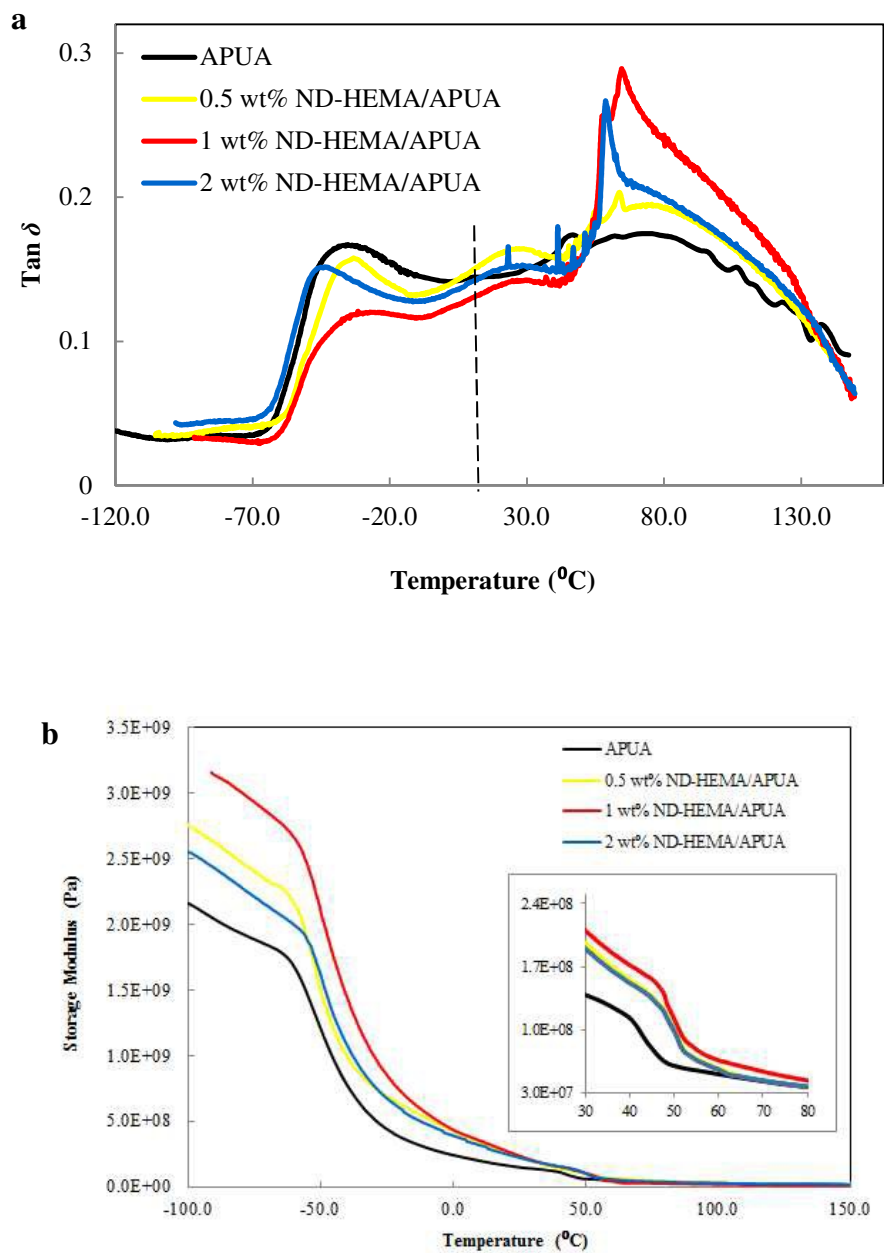


Fig. 7. DMA curves of APUA and APUA/ND-HEMA composites at frequency of 1 Hz (a) loss factor ($\tan \delta$) and (b) storage modulus.

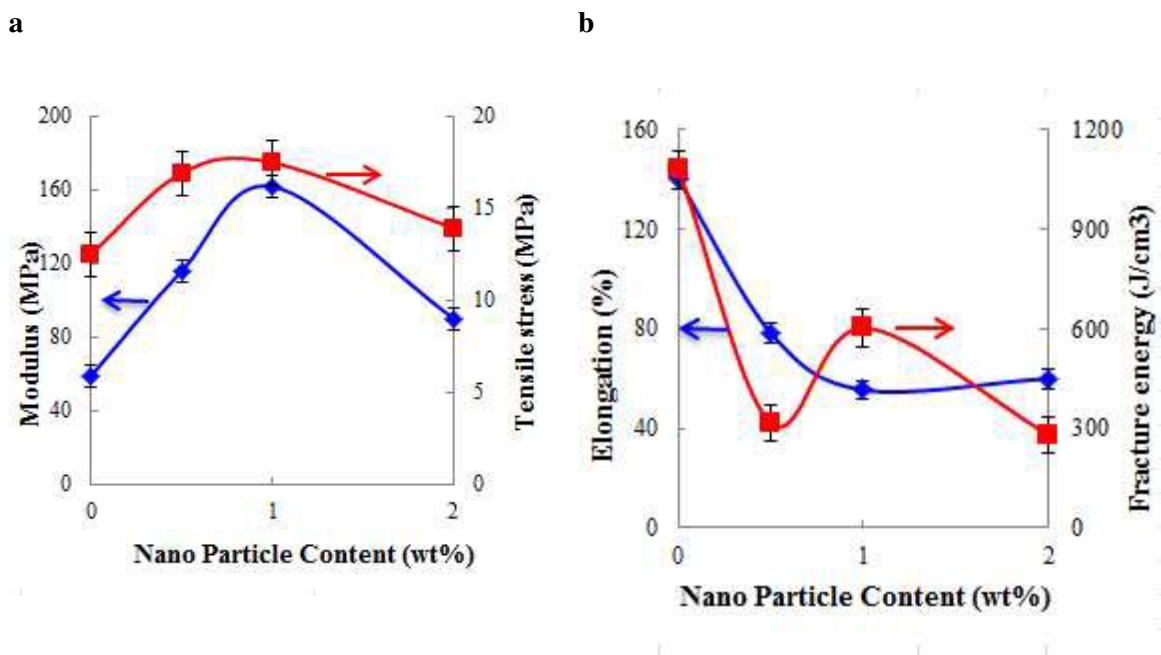


Fig 8. Tensile properties of the samples, a) modulus and tensile properties and b) elongation at break and fracture energy.

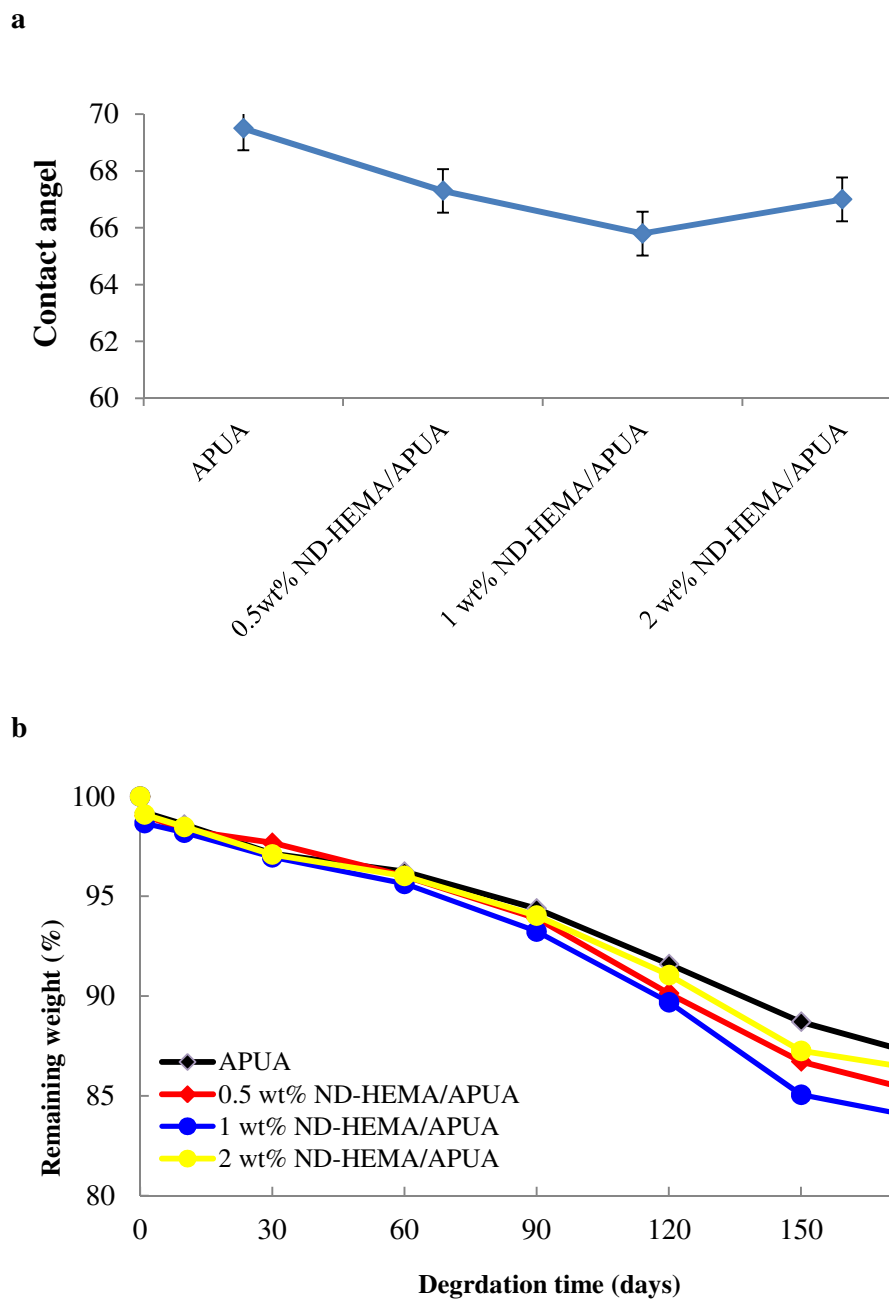


Fig 9. Contact angle (a) and degradation properties (b) of samples.

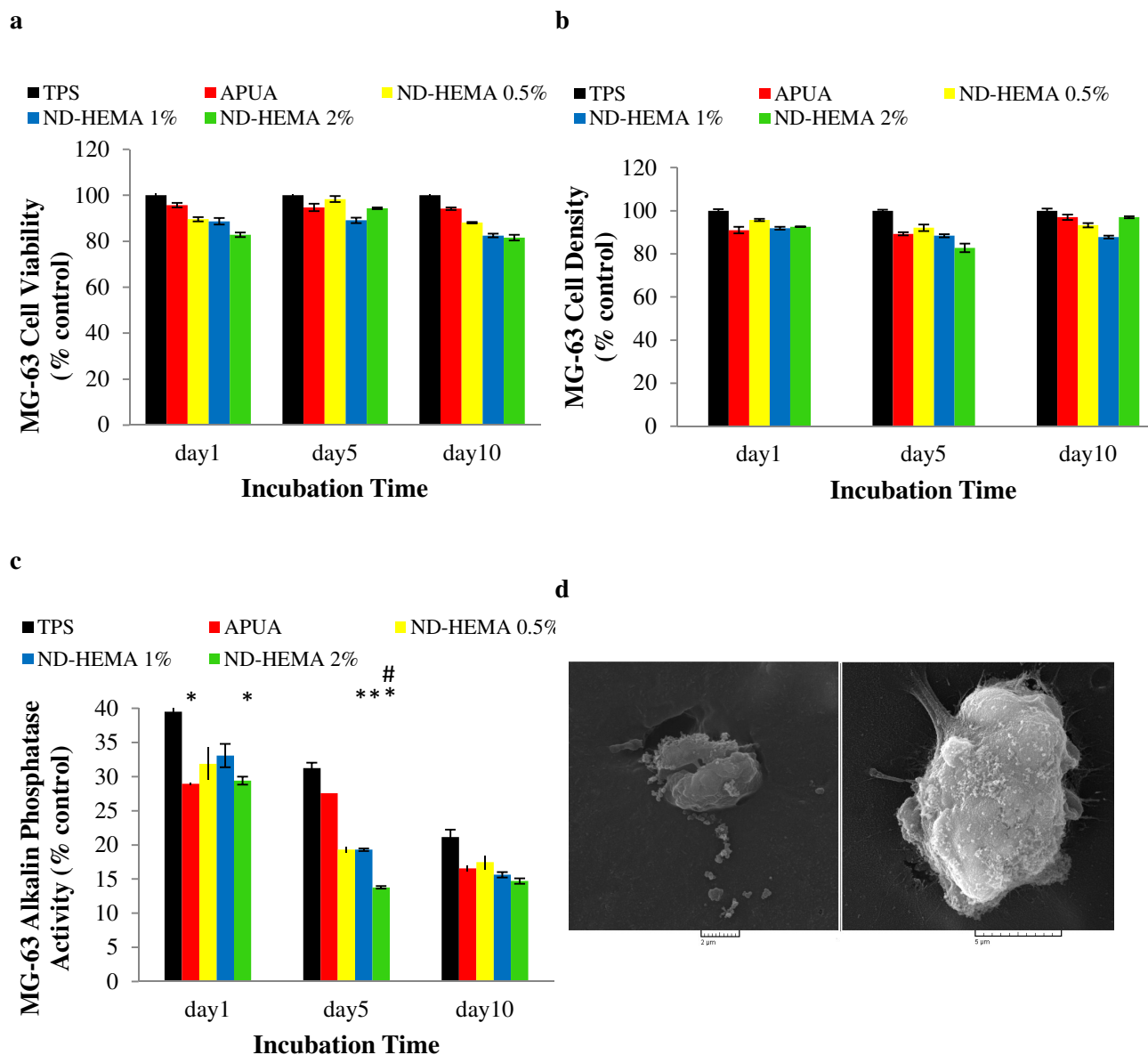


Fig. 10. Cellular behavior of neat APUA and APUA/ND-HEMA composites a) MTT viability; b) cell attachments; c) ALP activities. MG-63 osteoblast-like cells were cultured on the surface of APUA composites. (* Significant difference between TPS and APUA composites ($P < 0.05$), # Significant difference between APUA and composites ($P < 0.05$)) d) SEM microphotographs of MG-63 osteoblast-like cells cultured on the surface of APUA(left) and 1wt% composite (right).

Graphical Abstract

Biodegradable polyurethane acrylate/HEMA-grafted nanodiamond composites with bone regenerative potential applications: Structure, mechanical properties and biocompatibility

M. Alishiri, A. Shojaei, M. J. Abdekhodaie

It was found that ND-HEMA enhanced considerably the mechanical properties of biocompatible APUA at low concentrations, i.e. 1 wt%, while it retained the biocompatibility of the PAUA.

